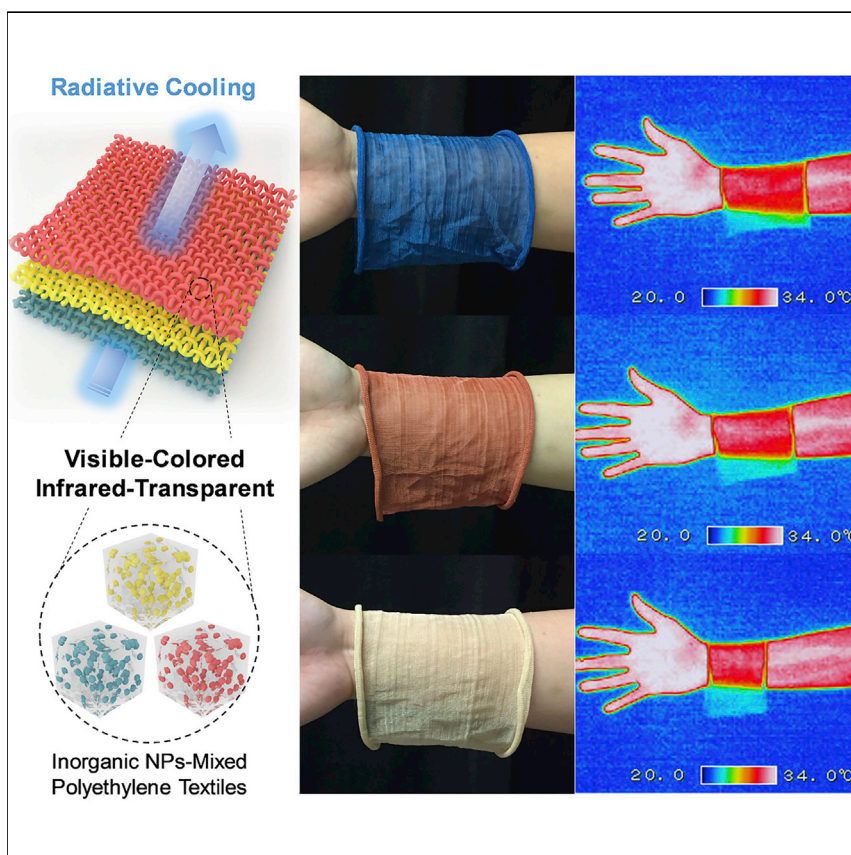


Article

Temperature Regulation in Colored Infrared-Transparent Polyethylene Textiles



Coloration of infrared-transparent polyethylene textiles is demonstrated to address the major challenge toward wide adoption of radiative cooling technology for personal thermal management. Utilizing inorganic pigment nanoparticles, such as Prussian blue, iron oxide, and silicon, infrared-transparent polyethylene fabrics of various colors are developed via scalable fabrication processes.

Lili Cai, Yucan Peng, Jinwei Xu, ..., Dingchang Lin, Shanhui Fan, Yi Cui

yicui@stanford.edu

HIGHLIGHTS

Inorganic NPs with negligible IR absorption are utilized as the coloring component

Colored PE fabrics are made by scalable compounding, extruding, and knitting processes

80% IR transparency and 1.6°C–1.8°C radiative cooling are achieved with diverse colors

Good stability against more than 100 washing cycles can be sustained

Article

Temperature Regulation in Colored Infrared-Transparent Polyethylene Textiles

Lili Cai,^{1,4} Yucan Peng,^{1,4} Jinwei Xu,¹ Chenyu Zhou,¹ Chenxing Zhou,¹ Peilin Wu,¹ Dingchang Lin,¹ Shanhui Fan,² and Yi Cui^{1,3,5,*}

SUMMARY

Effectively regulating heat flow between the human body and its environment not only increases thermal comfort but also presents a novel and potentially cost-effective approach to reducing building energy consumption. Infrared property-engineered textiles have been shown to passively regulate radiative heat dissipation for effective cooling and warming of the human body. However, a lack of dyes that can tune the textile color without compromising the infrared properties remains a major impediment to textile commercialization. Here, we report a new strategy utilizing inorganic nanoparticles as a coloring component for scalable brightly colored, infrared-transparent textiles. The as-fabricated composite textiles not only show a high infrared transparency of $\sim 80\%$ and a passive cooling effect of $\sim 1.6^\circ\text{C}$ – 1.8°C but also exhibit intense visible colors with good stability against washing. This facile coloration approach will promote the commercialization of radiative cooling textiles in temperature-regulating wearable applications for effective energy savings.

INTRODUCTION

Heat-flow management through wearable technology has the potential for improving human health and comfort. Furthermore, heat-managing wearables can result in substantial energy savings,¹ considering that extensive energy is consumed on space heating and cooling (for instance, more than 10% of the total energy consumption in the U.S.).^{2,3} In contrast to building-level temperature regulation where most of the energy is wasted on unoccupied space, personal thermal management is a more efficient and cost-effective alternative that aims to provide localized heating and cooling to the human body and its immediate environment.

Recent studies have found that controlling the infrared (IR) optical properties of garment textiles can have strong effects on localized cooling and heating of the human body.^{4–10} For example, IR-transparent nanoporous polyethylene (nanoPE) was demonstrated to passively cool the body by 2°C ,^{5,9} and metallized nanoPE with low IR emissivity can warm the body by 7°C .⁷ This is due to the fact that the human skin has high emissivity ($\epsilon = 0.98$) and acts like a black body,¹¹ strongly emitting thermal radiation in the IR wavelength range of 7–14 μm with a peak intensity at 9.5 μm .⁵ Therefore, thermal radiation plays an indispensable role in human-body heat dissipation, accounting for more than 50% of heat dissipation in indoor conditions.^{12,13} These findings opened a new direction for personal thermal management, as conventional textile materials lack the capability of infrared radiation control.

Context & Scale

Effective temperature regulation on wearables not only can improve human health and comfort but also hold great promise for energy savings. Recent reports of infrared-transparent polyethylene textiles showed passive cooling effect by allowing the thermal radiation from the human body to pass through, but they lacked the tunability in visible color. In this work, we demonstrate for the first time a strategy utilizing unique inorganic pigment nanoparticles to achieve coloration of infrared-transparent polyethylene textiles for radiative cooling. With the demonstrated scalable fabrication processes and good stability against washing, this work will enable us to move one step closer to practical application of energy-efficient and cost-effective radiative cooling textiles for personal thermal management.

However, effective infrared management of textiles is difficult while simultaneously controlling their visible color. This remains the major challenge that limits the application of infrared-engineered textiles in real life, as color selection is one of the most important factors that govern the wearable market.¹⁴ The chemical bonds that are characteristic to commonly used organic dye molecules strongly absorb human-body radiation in the mid-IR wavelength range, e.g., C-O stretching (7.7–10 μm), C-N stretching (8.2–9.8 μm), aromatic C-H bending (7.8–14.5 μm), and S=O stretching (9.4–9.8 μm).^{15,16} Thus, usage of organic dyes can cause low IR transparency and high IR emissivity, making them unsuitable for either radiative cooling or heating effects. Additionally, polyethylene, the base material for radiative cooling and heating textiles, is chemically inert and lacks polar groups, which inhibits surface adhesion of chemical dyes.^{17–19}

In this work, we provide a potential solution to the dilemma between visible and infrared optical properties and report the first demonstration of colored polyethylene textiles with high IR transparency for radiative cooling. We achieve this by successfully identifying and utilizing unique inorganic pigment nanoparticles that have negligible absorption in the IR region, while reflecting certain visible colors through optimized concentration and size. Compounding the inorganic pigment nanoparticles into the polyethylene matrix forms a uniform composite for stable coloration compared to the surface-adhesion approach, which was previously reported to have difficulty in achieving stable coloration for polyethylene.²⁰ We further demonstrate that the colored polyethylene composite can be readily extruded into mechanically strong, continuous fibers for knitting of interlaced fabrics using scalable processes. The knitted fabrics show not only high IR transparency of $\sim 80\%$ and good radiative cooling performance of 1.6°C–1.8°C but also good color stability against more than 100 washing cycles. This work lays the foundation for practical implementation of radiative cooling textiles to enable better personal thermal management for more efficient energy utilization.

RESULTS AND DISCUSSION

Coloration Design for Infrared-Transparent Polyethylene Textiles

The design schematic of the colored polyethylene textile is shown in Figure 1A. We chose IR-transparent inorganic nanoparticles as the pigment and polyethylene as the flexible polymer host. These two components were uniformly mixed via compounding and could then be extruded into fibers for weaving or knitting interlaced fabrics. The inorganic solids that we found to satisfy the requirement of IR transparency include Prussian blue (PB), iron oxide (Fe_2O_3), and silicon (Si), which are also non-toxic and low cost, as shown in Figure 1B. Fourier transform infrared (FTIR) spectroscopy (Figure 1C) illustrates that these inorganic solids have negligible absorbance in the infrared wavelength region of 4–14 μm , except for an intense and narrow peak of PB at 4.8 μm due to $\text{C}\equiv\text{N}$ stretching vibration and a weak and broad peak of silicon around 8–10 μm due to the native silicon oxide on the surface. In contrast, traditional organic dye molecules show significantly more IR absorption peaks. Their particle sizes were in the range of 20–1,000 nm, as revealed in the scanning electron microscopy (SEM) images in Figures 1D–1F. On one hand, this nanoscale size range is much smaller than the human-body thermal radiation wavelengths of 4–14 μm ; hence, these nanoparticles will not strongly scatter infrared light to decrease the IR transparency of the colored polyethylene mixtures.²¹ On the other hand, high refractive index dielectric or semiconductor nanoparticles in a particular size range can have strong resonant light scattering in the visible spectral range on the basis of Mie theory.^{21–23} Therefore, different colors can be produced by

¹Department of Materials Science and Engineering, Stanford University, Stanford, CA 94305, USA

²E. L. Ginzton Laboratory, Department of Electrical Engineering, Stanford University, Stanford, CA 94305, USA

³Stanford Institute for Materials and Energy Sciences, SLAC National Accelerator Laboratory, 2575 Sand Hill Road, Menlo Park, CA 94025, USA

⁴These authors contributed equally

⁵Lead Contact

*Correspondence: yicui@stanford.edu
<https://doi.org/10.1016/j.joule.2019.03.015>

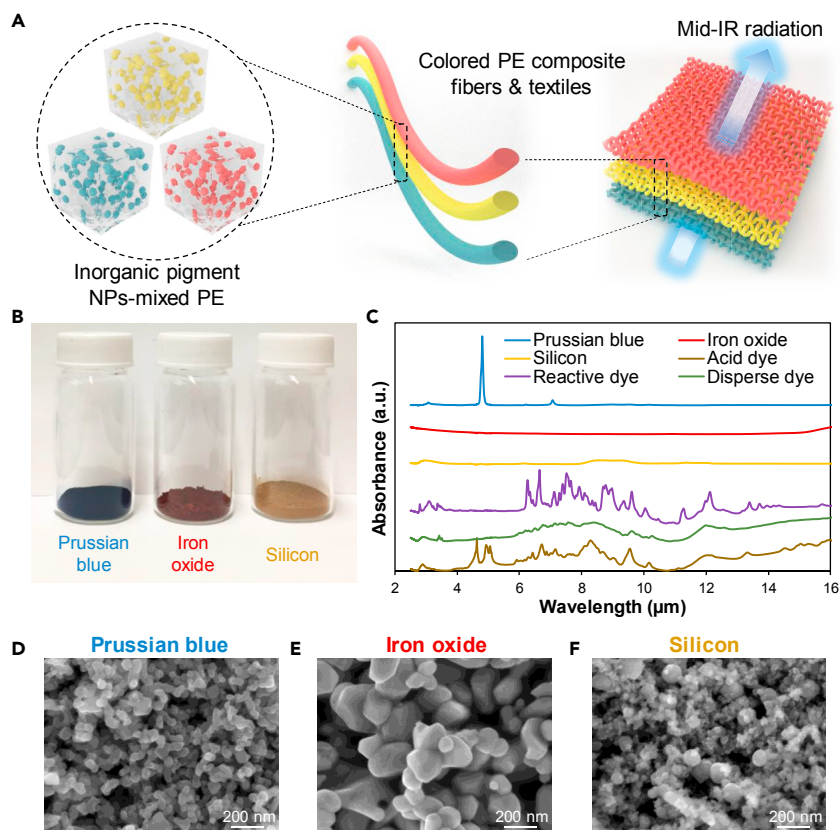


Figure 1. Coloration Design for Infrared-Transparent Polyethylene Textiles

(A) Design schematic for the coloration of radiative cooling textiles, which is made by mixing IR-transparent inorganic pigment nanoparticles with polyethylene (PE). The mixed composites can then be extruded into continuous fibers for knitting into interlaced textiles via large-scale industrial processes.

(B) Photograph of the selected inorganic pigment powders.

(C) FTIR absorbance spectra comparison between the selected inorganic pigment particles and traditional organic dye molecules.

(D–F) SEM images of the nanoparticles for (D) Prussian blue, (E) iron oxide, and (F) silicon.

controlling the nanoscale dimensions. For example, in contrast to the black color of bulk silicon, silicon nanoparticles (refractive index > 3.8 at 633 nm) with diameters of 100–200 nm are yellow, which results from pronounced Mie resonance responses associated with the excitation of both magnetic and electric dipole modes.^{24–26} Different from silicon nanoparticles, both PB and iron oxide nanoparticles show the same colors as their natural bulk counterparts.²⁷ The intense blue color of PB is associated with the intervalence charge transfer between Fe(II) and Fe(III),^{28,29} while the dark red color of iron oxide is determined by its band gap of ~ 2.2 eV.^{30,31} With these three primary colors of blue, red, and yellow, arbitrary colors over the whole visible spectrum can be created by mixing them at different ratios. For example, we were able to produce a green color by mixing Si and PB in the mass ratio of 1:1, as shown in Figure S1.

Fabrication of Inorganic Pigment-Embedded Polyethylene Composites

The compounding process was employed to mechanically mix the nanoparticles with melted polyethylene pellets at 180°C, which produces uniform inorganic solid-polymer composites. The minimum mass ratio of pigments needed to

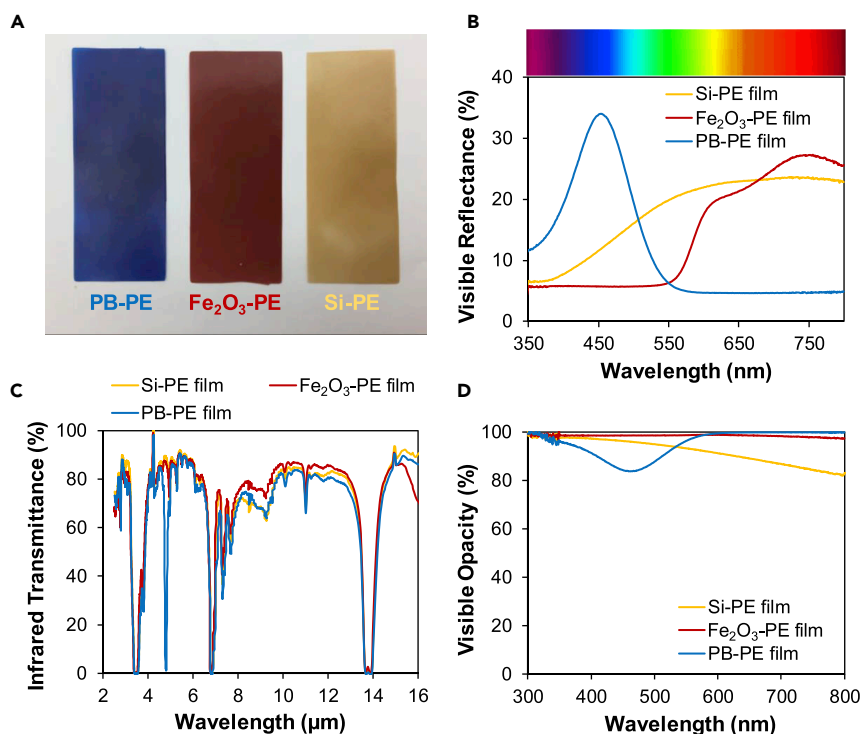


Figure 2. Fabrication and Optical Properties of Inorganic Pigment-Embedded Polyethylene Composites

(A) Photograph, (B) UV-VIS reflectance, (C) FTIR transmittance, and (D) visible opacity spectra of the pigment nanoparticle-mixed polyethylene composite films.

achieve high opacity (>80%) and observable colors (peak reflectance > 20%) for the mixed composites was found to be about 1%. With a mass ratio of 1% nanoparticles, the composites maintain good thermal processability for molding into arbitrary shapes and satisfactory optical properties for both visible and infrared wavelength ranges. Due to the uniform distribution of pigment nanoparticles inside the polyethylene polymer matrix, the 100- μm -thick molded PB-PE, Fe₂O₃-PE, and Si-PE composite films show uniform and intense coloration of blue, red, and yellow, respectively (Figure 2A). The ultraviolet-visible (UV-VIS) spectroscopy measurement of the composite films reveals dominant reflection wavelengths around 450 nm, 600 nm, and 750 nm, matching well to the original colors of PB, iron oxide, and silicon nanoparticles, respectively (Figure 2B). The strong reflection and absorption of visible light lead to high opacity (defined as $1 - \text{specular transmittance}$) of more than 80% in the visible range (Figure 2D); this satisfies one of the basic functions of clothing: preventing the object behind the textile from being recognized. Furthermore, in the mid-IR region, the composites all show high transparency of $\sim 80\%$ (Figure 2C), allowing high transmittance of body radiation heat for achieving radiative cooling. It should be noted that the nanoparticle concentration does not affect the IR transparency of the composite, since these nanoparticles do not absorb radiation in the mid-IR spectral range. As the nanoparticle concentrations increase to 5% and even 10%, the composites maintain high IR transparency (Figure S2). Therefore, these inorganic pigments provide flexibility in color tuning without compromising their thermal properties. In comparison, the adverse effect of traditional organic dyes on IR transparency is exacerbated as their concentration increases.

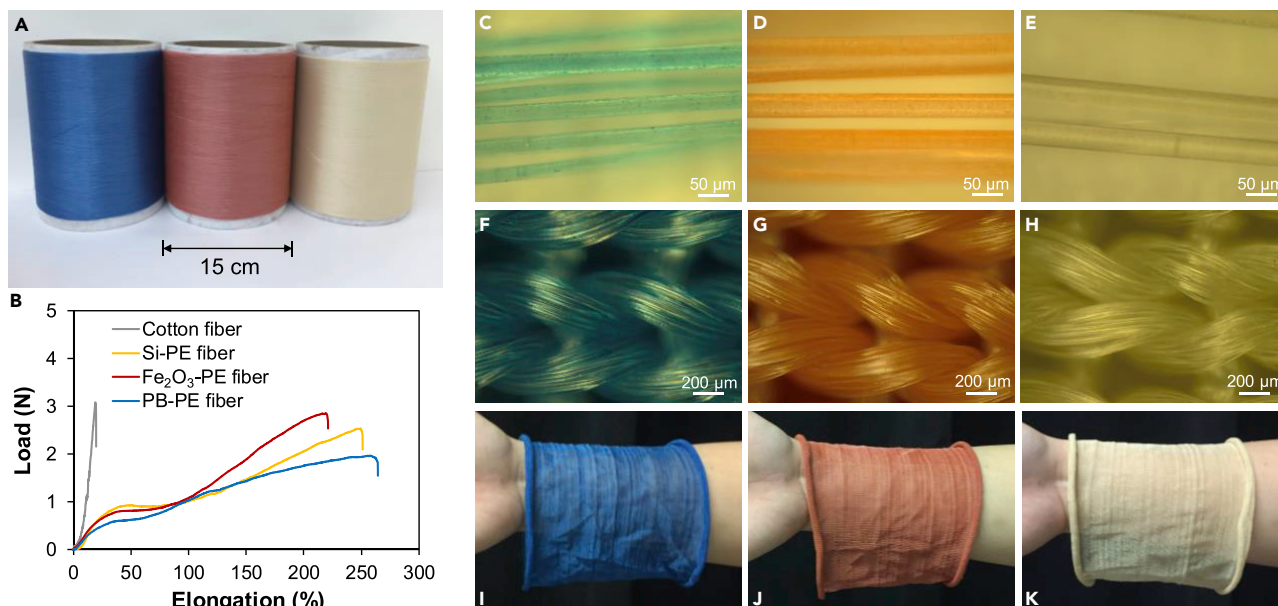


Figure 3. Fabrication of Colored Polyethylene Fibers and Textiles

(A) Photograph of three spools of the colored polyethylene fibers produced by industrial extrusion. (B) Tensile strength test demonstrates that the colored polyethylene fibers have tensile strength comparable to that of cotton. (C–E) Optical micrographs of the extruded fibers for (C) blue PB-PE, (D) red Fe_2O_3 -PE, and (E) yellow Si-PE. (F–H) Optical micrographs showing the knitting pattern for (F) blue PB-PE, (G) red Fe_2O_3 -PE, and (H) yellow Si-PE. (I–K) Photographs of the knitted textiles with good wearability for (I) blue PB-PE, (J) red Fe_2O_3 -PE, and (K) yellow Si-PE.

Characterization of Colored Polyethylene Fibers and Textiles

We further demonstrated the extrusion of colored polyethylene composites into multi-filament yarns using a high-throughput melt-spinning machine (Figure 3A). Each extruded yarn consists of 19 single-filament fibers with diameter of ~ 30 – $50 \mu\text{m}$, as revealed by optical micrographs in Figures 3C–3E. It is also evident that the pigment nanoparticles are uniformly embedded inside the fibers. In addition, mechanical strength tests show that the colored polyethylene composite yarns can sustain a maximum tensile force of ~ 1.9 – 2.8 N , which is comparable to the cotton yarn used in normal clothing fabrics (Figure 3B). The decent mechanical strength enabled further knitting of the yarns into large-scale interlaced fabrics with good breathability, softness, and mechanical strength (Figures 3F–3K). Even with further processing into interlaced knits, the colored polyethylene composite fabrics still show high infrared transmittance of $\sim 80\%$ (Figure 4A), similar to that of the planar solid films shown in Figure 2C. The stability and durability of the colored polyethylene fabrics were evaluated by measuring the Fe, K, and Si ion concentrations in water before and after washing with detergent using inductively coupled plasma mass spectrometry. The fractions of the total pigment mass that were lost over 1 washing cycle and 120 washing cycles are calculated and shown in Figure 4B. Much of the loss occurred in the first wash cycles ($< 3\%$), which likely arises from partially exposed particles on the fiber surface, while successive washing cycles result in minimal further loss ($< 3.6\%$ after 120 cycles). This confirms that the Fe_2O_3 , PB, and Si nanoparticles are firmly embedded in the polyethylene polymer matrix, which can sustain washing and maintain the original optical properties (Figure S3) without releasing pigment nanoparticles into the water.

Thermal Measurement

Finally, we characterized the thermal performance of the colored polyethylene textiles. A rubber insulated flexible heater with IR emissivity similar to that of human skin

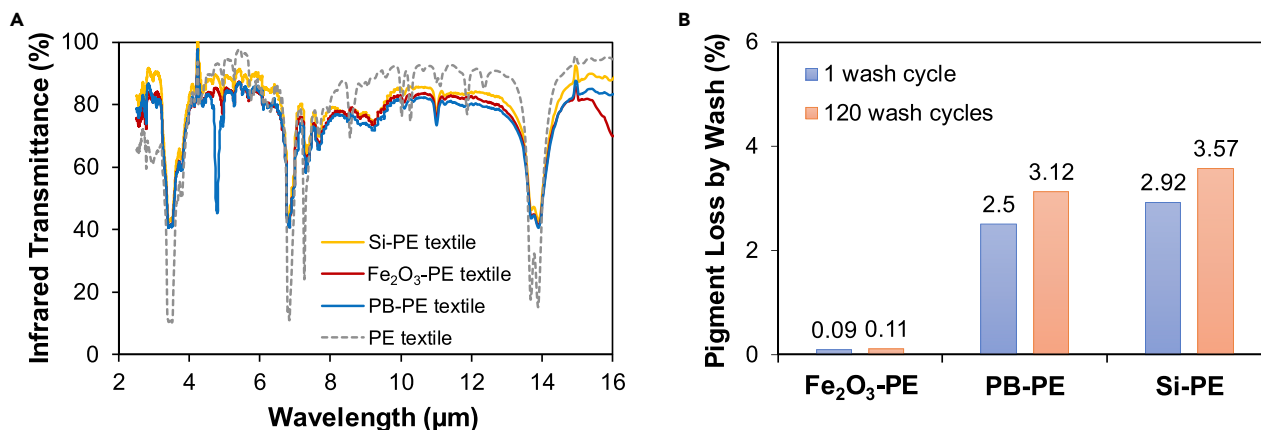


Figure 4. Characterization of Infrared Transmittance and Washing Stability

(A) Measured total FTIR transmittance of the colored polyethylene textiles and uncolored nanoporous polyethylene textiles.

(B) Chart showing the pigment mass loss percentage after washing the colored polyethylene textiles in the water with detergent.

(Figure S4) was used to simulate human heat generation. The temperature response of the model skin was recorded when covered with different textile samples. The whole set-up was enclosed in a chamber where the convection effect is minimized, and the surrounding air temperature inside the chamber was maintained constant at 25°C. At a heating power density of 80 W m⁻², comparable to the human-body metabolic heat generation rate, the bare skin heater showed a temperature of 33.5°C.³² When the skin heater was covered with a normal cotton textile, the skin temperature increased to 36.5°C (Figure 5A). When covered with the PB-PE, Fe₂O₃-PE, and Si-PE textiles, the skin temperatures were measured in the range of ~34.7°C–34.9°C, demonstrating their capability to passively cool human skin by 1.6°C–1.8°C as compared to cotton. These experimental results are in good agreement with heat-transfer modeling of the infrared cooling effect in previous works.^{4,5} This cooling effect is similar to that of the previously reported undyed nanoPE,^{5,9} which further confirms the effectiveness of IR-transparent pigment nanoparticles for the coloration of radiative cooling textiles. We also used an infrared camera to visualize and validate the radiative cooling effect while wearing the colored polyethylene textiles on the human skin (Figure 5B). The comparison under thermal imaging clearly illustrates that the colored polyethylene textiles allow superior transmission of the body radiation heat to the environment compared to normal cotton textiles.

In summary, we demonstrated a novel approach based on inorganic pigment nanoparticles for large-scale fabrication of visible-colored and infrared-transparent textiles, which can allow efficient dissipation of human-body radiation while exhibiting diverse colors as found in conventional textiles. The pigment materials of PB, iron oxide, and silicon generate primary colors of blue, red, and yellow, respectively, while maintaining negligible IR absorption, non-toxicity, and low cost. Arbitrary colors over the visible spectrum can be potentially created by mixing these three pigments at different ratios. Through scalable compounding, extrusion, and knitting processes with optimized nanoparticle concentration and size, the as-fabricated composite textiles show intense visible colors, high infrared transparency of ~80%, passive cooling effect of 1.6°C–1.8°C, and good washing stability. The work presented here solves a key bottleneck in the coloration of radiative cooling textiles to move closer to practical applications of energy-efficient and cost-effective wearable technologies for personal thermal management.

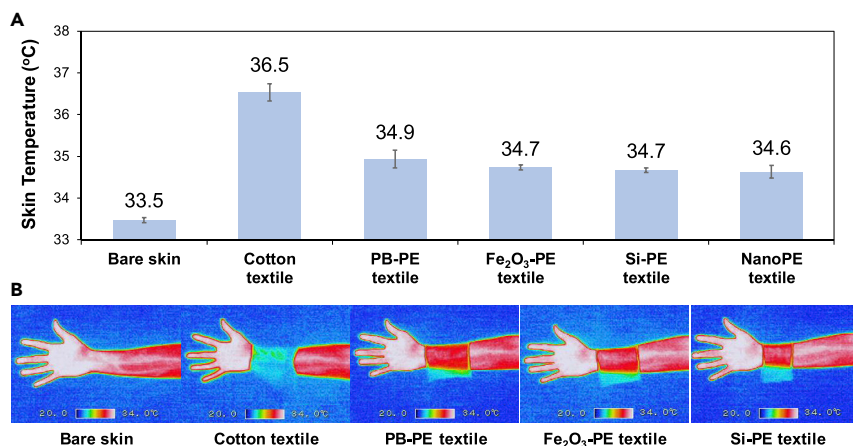


Figure 5. Thermal Measurement

(A) Comparison of the temperatures measured with bare and textile-covered skin-simulating heaters. Textile samples include cotton, PB-PE, Fe₂O₃-PE, Si-PE, and nanoPE.

(B) Infrared images of bare skin and human skin covered with cotton, PB-PE, Fe₂O₃-PE, and Si-PE textiles.

EXPERIMENTAL PROCEDURES

Textile Fabrication

Pigmented polyethylene was made by mixing inorganic solid pigment nanoparticles such as PB (ACROS Organics), iron oxide (Sigma-Aldrich, 99%), and silicon (MTI Corporation, 100 nm, 99%) with melted high-density polyethylene pellets (melt index: 2.2 g per 10 min, Sigma-Aldrich) at 180°C using a twin-screw compounder (Polymers Center of Excellence). The mass ratio of nanoparticles and polyethylene is 1:100. The nanoparticle-mixed polyethylene composites were then extruded into fibers using a multi-filament melt-spinning machine (Hills, Inc.). Textile knitting was conducted using a FAK sampler knitting machine at the Textile Technology Center of Gaston College.

Material Characterization

Micrographs of the extruded fibers and knitted textiles were taken with an optical microscope (Olympus). SEM images were acquired by a FEI XL30 Sirion SEM at an accelerating voltage of 5 kV. The infrared absorbance and transmittance were measured using an FTIR spectrometer (Model 6700, Thermo Scientific) with a diffuse gold integrating sphere (PIKE Technologies). The visible reflection and opacity were measured by an ultraviolet-visible spectrometer (Agilent, Cary 6000i).

Thermal Measurement

Skin was simulated using a rubber insulated flexible heater (Omega, 72 cm²), which was connected to a power supply (Keithley 2400). A ribbon-type hot junction thermocouple (0.3 mm in diameter, K-type, Omega) was contacted with the top surface of the simulated skin to measure the skin temperature. A guard heater and insulating foam were placed below the simulated skin heater to ensure that the heat generated by the skin heater was only transferred to the ambient. The temperature of the guard heater was always set the same as the skin heater, so downward heat conduction to the table was averted. The whole device was enclosed in a chamber, and the temperature inside the chamber was controlled to be constant at 25°C. We set the power density of the skin heater to be constant at 80 W m⁻², which rendered a skin temperature of 33.5°C at an ambient temperature of 25°C. When the skin was covered by

the textile sample ($5 \times 5 \text{ cm}^2$), we measured the steady-state skin temperature response while the ambient temperature was maintained at 25°C . Thermal images were taken by a calibrated thermal camera (MikroSHOT, Mikron). The cotton textile sample is commercially available (single jersey knit, 130 g per square meter).

Mechanical Test

The tensile strength test was measured by Instron 5565. The yarn samples were cut to a length of 4 cm. The gauge distance was 2 cm long, and the displacement rate was kept at 10 mm min^{-1} . The cotton yarn for mechanical tests was taken from a commercial cotton textile (single jersey cotton, 130 g per square meter).

Washing Test

The knitted textiles were washed in water (60 mL) with detergent (2 mL) under stirring at the speed of 500 rpm for 30 min (equivalent to 1 wash cycle) and 60 h (equivalent to 120 wash cycles). The water before and after wash was collected and then tested using inductively coupled plasma mass spectrometry (ICP-MS) to quantify the amount of metal ions (K, Fe, and Si for PB, iron oxide, and silicon, respectively) that were released from the textile samples during washing.

SUPPLEMENTAL INFORMATION

Supplemental Information can be found online at <https://doi.org/10.1016/j.joule.2019.03.015>.

ACKNOWLEDGMENTS

This work was sponsored by the Advanced Research Projects Agency-Energy (ARPA-E), U.S. Department of Energy, under Award Number DE-AR0000533. We acknowledge William Huang and Allen Pei for copyediting the manuscript.

AUTHOR CONTRIBUTIONS

L.C. and Y.C. conceived the idea. L.C. carried out all the experiments with the assistance of Y.P., J.X., Chenyu Zhou, Chenxing Zhou, and P.W. D.L. drew the schematic. S.F. and Y.C. supervised the project. L.C. and Y.C. wrote the paper. All authors discussed the results and commented on the manuscript.

DECLARATION OF INTERESTS

The authors have filed a U.S. non-provisional patent application (US 16/267242) and an international patent application (PCT/US19/16554) related to this work.

Received: December 9, 2018

Revised: February 13, 2019

Accepted: March 14, 2019

Published: March 21, 2019

REFERENCES

1. Hoyt, T., Arens, E., and Zhang, H. (2015). Extending air temperature setpoints: Simulated energy savings and design considerations for new and retrofit buildings. *Build. Environ.* 88, 89–96.
2. Pérez-Lombard, L., Ortiz, J., and Pout, C. (2008). A review on buildings energy consumption information. *Energy Build.* 40, 394–398.
3. Office of Energy Efficiency and Renewable Energy (EERE). (2011). *Buildings Energy Data Book*. <https://openei.org/doe-opendata/dataset/buildings-energy-data-book>.
4. Tong, J.K., Huang, X., Boriskina, S.V., Loomis, J., Xu, Y., and Chen, G. (2015). Infrared-transparent visible-opaque fabrics for wearable personal thermal management. *ACS Photonics* 2, 769–778.
5. Hsu, P.-C., Song, A.Y., Catrysse, P.B., Liu, C., Peng, Y., Xie, J., Fan, S., and Cui, Y. (2016). Radiative human body cooling by nanoporous polyethylene textile. *Science* 353, 1019–1023.
6. Catrysse, P.B., Song, A.Y., and Fan, S. (2016). Photonic structure textile design for localized thermal cooling based on a fiber blending scheme. *ACS Photonics* 3, 2420–2426.

7. Cai, L., Song, A.Y., Wu, P., Hsu, P.-C., Peng, Y., Chen, J., Liu, C., Catrysse, P.B., Liu, Y., Yang, A., et al. (2017). Warming up human body by nanoporous metallized polyethylene textile. *Nat. Commun.* **8**, 496.
8. Hsu, P.-C., Liu, C., Song, A.Y., Zhang, Z., Peng, Y., Xie, J., Liu, K., Wu, C.-L., Catrysse, P.B., Cai, L., et al. (2017). A dual-mode textile for human body radiative heating and cooling. *Sci. Adv.* **3**, e1700895.
9. Peng, Y.C., Chen, J., Song, A.Y., Catrysse, P.B., Hsu, P.C., Cai, L.L., Liu, B.F., Zhu, Y.Y., Zhou, G.M., Wu, D.S., et al. (2018). Nanoporous polyethylene microfibrils for large-scale radiative cooling fabric. *Nature Sustainability* **1**, 105–112.
10. Cai, L., Song, A.Y., Li, W., Hsu, P.-C., Lin, D., Catrysse, P.B., Liu, Y., Peng, Y., Chen, J., Wang, H., et al. (2018). Spectrally selective nanocomposite textile for outdoor personal cooling. *Adv. Mater.* **30**, e1802152.
11. Steketee, J. (1973). Spectral emissivity of skin and pericardium. *Phys. Med. Biol.* **18**, 686–694.
12. Hardy, J.D., and Dubois, E.F. (1937). Regulation of heat loss from the human body. *Proc. Natl. Acad. Sci. USA* **23**, 624–631.
13. Winslow, C.-E., Gagge, A., and Herrington, L. (1939). The influence of air movement upon heat losses from the clothed human body. *American Journal of Physiology—Legacy Content* **127**, 505–518.
14. Marshall, S.G., Jackson, H.O., Stanley, M.S., Kefgen, M., and Touchie-Specht, P. (2012). *Individuality in Clothing Selection and Personal Appearance* (Pearson Prentice Hall).
15. Matsuoka, M. (2013). *Infrared Absorbing Dyes* (Springer).
16. Lee, J., Kang, M.H., Lee, K.-B., and Lee, Y. (2013). Characterization of natural dyes and traditional Korean silk fabric by surface analytical techniques. *Materials (Basel)* **6**, 2007–2025.
17. Brewis, D.M., and Briggs, D. (1981). Adhesion to polyethylene and polypropylene. *Polymer (Guildf.)* **22**, 7–16.
18. Kim, T., Jeon, S., Kwak, D., and Chae, Y. (2012). Coloration of ultra high molecular weight polyethylene fibers using alkyl-substituted anthraquinoid blue dyes. *Fibers Polym.* **13**, 212–216.
19. Nardin, M., and Ward, I.M. (1987). Influence of surface treatment on adhesion of polyethylene fibres. *Mater. Sci. Technol.* **3**, 814–826.
20. Park, S.-J., Song, S.-Y., Shin, J.-S., and Rhee, J.-M. (2005). Effect of surface oxyfluorination on the dyeability of polyethylene film. *J. Colloid Interface Sci.* **283**, 190–195.
21. Bohren, C.F., and Huffman, D.R. (2008). *Absorption and Scattering of Light by Small Particles* (Wiley).
22. Zhao, Q., Zhou, J., Zhang, F., and Lippens, D. (2009). Mie resonance-based dielectric metamaterials. *Mater. Today* **12**, 60–69.
23. Evlyukhin, A.B., Reinhardt, C., Seidel, A., Luk'yanchuk, B.S., and Chichkov, B.N. (2010). Optical response features of Si-nanoparticle arrays. *Phys. Rev. B* **82**, 045404.
24. Evlyukhin, A.B., Novikov, S.M., Zywiets, U., Eriksen, R.L., Reinhardt, C., Bozhevolnyi, S.I., and Chichkov, B.N. (2012). Demonstration of magnetic dipole resonances of dielectric nanospheres in the visible region. *Nano Lett.* **12**, 3749–3755.
25. Kuznetsov, A.I., Miroshnichenko, A.E., Fu, Y.H., Zhang, J., and Luk'yanchuk, B. (2012). Magnetic light. *Sci. Rep.* **2**, 492.
26. Zywiets, U., Evlyukhin, A.B., Reinhardt, C., and Chichkov, B.N. (2014). Laser printing of silicon nanoparticles with resonant optical electric and magnetic responses. *Nat. Commun.* **5**, 3402.
27. Shevell, S.K. (2003). *The Science of Color* (Elsevier Science).
28. Samain, L., Grandjean, F., Long, G.J., Martinetto, P., Bordet, P., and Strivay, D. (2013). Relationship between the synthesis of prussian blue pigments, their color, physical properties, and their behavior in paint layers. *J. Phys. Chem. C* **117**, 9693–9712.
29. Rosseinsky, D.R., Lim, H., Jiang, H., and Chai, J.W. (2003). Optical charge-transfer in iron(III) hexacyanoferrate(II): electro-intercalated cations induce lattice-energy-dependent ground-state energies. *Inorg. Chem.* **42**, 6015–6023.
30. Gilbert, B., Frandsen, C., Maxey, E.R., and Sherman, D.M. (2009). Band-gap measurements of bulk and nanoscale hematite by soft x-ray spectroscopy. *Phys. Rev. B* **79**, 035108.
31. Kerker, M., Scheiner, P., Cooke, D.D., and Kratochvil, J.P. (1979). Absorption index and color of colloidal hematite. *J. Colloid Interface Sci.* **71**, 176–187.
32. Gagge, A.P., and Nishi, Y. (2011). Heat exchange between human skin surface and thermal environment. *Compr. Physiol. Supplement* **26**, 69–92.